22 *Inorg. Chem.* **2011**, *50*, 22–29
DOI: 10.1021/ic100803m

Inorganic Chemistry
Article

Computational Insight into the Rh-Mediated Activation of White Phosphorus

Wolfgang W. Schoeller*,†,‡

†*Department of Chemistry University of California at Riverside, Riverside, California 92521-0403, United States, and* ‡*Faculty of Chemistry, University of Bielefeld, 33615 Bielefeld, Germany*

Received April 23, 2010

Density functional calculations on the reaction of white phosphorus with the ligand bis(diphenylphosphino)methyl (dppm) at a rhodium center are presented. The cationic transition metal fragment can react as a nucleophilic as well as an electrophilic species, driven by a simple twisting of the four-membered rings. As a consequence of the conformational controlled philicity, the insertion reaction into white phosphorus occurs with a small energy barrier. The white phosphorus tetrahedron can be chelated by two cationic transition metal fragments into an opened bicyclobutane moiety, strongly stabilized by π-stacking interactions of the phenyl groups at the two transition metal fragments. It causes a 2:1 coordination; in the first stage of the reaction two molecules of the fragment add to one molecule of white phosphorus. The resulting dicationic complex easily undergoes dissociation into a cationic monoaddition product plus one cationic transition metal fragment. The ring expansion reaction of one ligand is explained by a j-step mechanism in one intermediary product. One ligand of the transition metal fragment dissociates and facilitates, by a cascade of low-energy processes, the rearrangement of the P_4-moiety. Under bipyramid formation a PP-bond is broken, and the free ligand finally attaches to one phosphorus atom. Overall the reaction can be divided in low-energy processes, which pass through different unstable intermediates and more high-energy processes, requiring ligand dissociation.

Introduction

Experimental studies on the degradation of white phosphorus with transition metals are legend, as revealed by numerous review articles on this subject.[1−3] A vast diversity of bonding situations is obtained, ranging from activation of P_4 by opening one or more edges or functionalization as a monohapto or dihapto ligand. A crucial experiment for understanding the white phosphorus degradation with transition metal fragments has been reported recently by Yakhvarov and Peruzzini et al.[4] (Scheme 1)

The reaction of the cationic transition metal complex $[M(dppm)_2]^+$ (M = Rh, **1-Rh** or Ir, **1-Ir**; dppm = PPh_2-CH_2PPh_2,[5] counteranion = OTf (trifluoromethanesulfonate)) was carried out at (a) low temperature (−40 °C) or at (b) room temperature (RT). Depending on the various reaction conditions, different results were obtained. At low temperature, exclusively the compound **3** was found. However, this path could only be verified for the Ir-derivative, **3-Ir**. At RT, a further product, **4-Rh** or **4-Ir** was observed. The Ir-derivative was also obtained by starting the reaction from **3-Ir**. While **3** and **4** are structurally characterized by X-ray investigations, **2-Ir** remains open for discussion. No structural evidence could be given for the latter.

The reaction of the transition metal fragment **1** with white phosphorus can be considered as an important finding, since it is one of the reactions that reveals characteristic features of a more general aspect for this type of chemistry, namely, two fragment molecules react at the same time with one molecule of white phosphorus. This 2:1 ratio has been observed for other phosphorus degradation reactions as well, for example, for the reaction of P_4 and its analogues As_4 with silylenes,[6,7] or with an aluminum based carbene analogue.[8] The present publications has a bearing on two aspects: (a) the mechanism of the reaction of **1** (M = Rh) with P_4, it will be revealed that electronic *and* steric effects govern the outcome of the reaction; (b) a general model will be presented for the 2:1 effect, where two fragments react with one P_4 molecule. The present analysis is based on modern quantum chemical density functional methods, procedures which can adequately account for the van der Waals interactions in sterically encumbered

*E-mail: wolfgang.schoeller@ucr.edu or wolfgang.schoeller@uni-bielefeld.de.

(1) (a) Caporali, M.; Gonsalvi, L.; Rossin, A.; Peruzzini, M. *Chem. Rev.* **2010**, *110*, 4178–4235. (b) Peruzzini, M.; Gonsalvi, L.; Romerosa, A. *Chem. Soc. Rev.* **2005**, *34*, 1038–1047.
(2) Whitmire, K. H. *Adv. Organomet. Chem.* **1998**, *42*, 1–145.
(3) (a) Scherer, O. J. *Acc. Chem. Res.* **1999**, *32*, 751–762. (b) Scherer, O. J. *Angew. Chem.* **1985**, *97*, 905–924.
(4) Yakhvarov, D.; Barbaro, P.; Gonsalvi, L.; Mañaz Carpio, S.; Midollini, S.; Orlandini, A.; Peruzzini, M.; Sinyashin, O.; Zanobini, F. *Angew. Chem., Int. Ed.* **2006**, *45*, 4182–4185.
(5) Hewertson, W.; Watson, H. R. *J. Chem. Soc.* **1962**, *12*, 1490–1494.
(6) Fanta, A. D.; Tan, R. P.; Comerlato, N. M.; Driess, M.; Powell, D. R.; West, R. *Inorg. Chim. Acta* **1992**, *198−200*, 733–739.
(7) Driess, M.; Fanta, A. D.; Powell, D.; West, R.. *Angew. Chem.* **1989**, *101*, 1087–1088.
(8) Peng, Y.; Fan, H.; Zhu, H.; Roesky, H. W.; Magull, J.; Hughes, C. E. *Angew. Chem., Int. Ed.* **2004**, *43*, 3443–3445.

 Published on Web 12/01/2010

Scheme 1

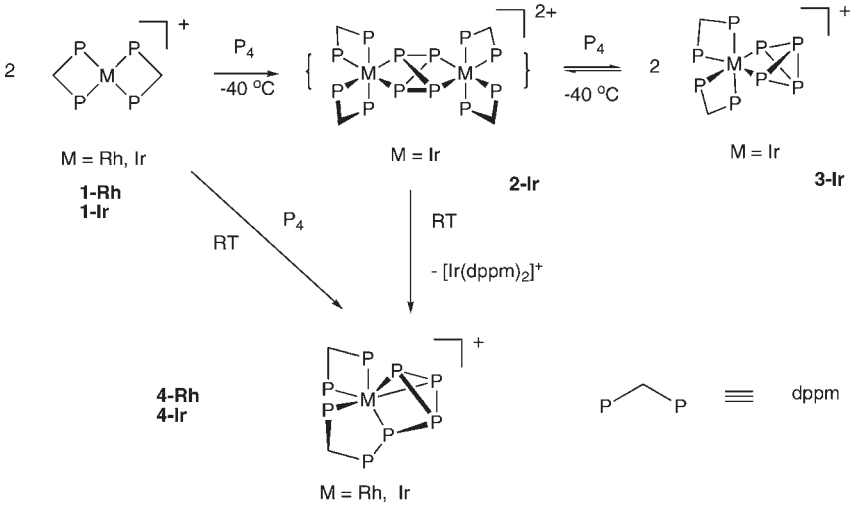

structures. Details of the quantum chemical procedures are summarized in the Section on quantum chemical procedures. Further results, like the equilibrium geometries of the most important structures are collected in the Supporting Information.

Results and Discussion

a. Through Bond versus through Space Isomerism in P_4. The molecular orbital system of tetrahedral P_4 is quite well established,[9−11] and an analogy to the molecular orbital system of PH_3[12] can be drawn. It gives rise to the assertion that the tetrahedron of P_4 prefers a peculiar position when a nucleophilic (Nu) or electrophilic (El) species approaches the ring system,[13] shown in Scheme 2.

In approach (**i**), one lone pair at the phosphorus tetrahedron will be coordinated, forming a σ-complex (n→p* electron transfer from the lone pair to the π^* orbital) with the transition metal fragment **1**. Alternatively, in approach (**j**) electron density will be shifted from the PP-bond to an approaching electrophile and in approach (**k**) from the nucleophile to the P-atom (of P_4). These simple considerations are quite well substantiated by studies on the reactivities of electrophilic (**j**) silylenes and/or nucleophilic (**k**) carbenes.[13] There the electrophilic or nucleophilic center is confined to one main group atom, either carbon (in a carbene) or silicon (in a silylene). Does this also hold for the P_4-case studied here? It will be shown that the degradation of P_4 with **1** can be rationalized by similar considerations. The essential difference to carbene or silylene chemistry is that the cationic fragment **1** exerts *conformational controlled philicity* (vide infra).

While the present considerations apply to first order rules for the treatment of the reactivity of P_4, one aspect needs further elaboration in the present discussion. The stretching of one PP-bond, as anticipated in Scheme 3, causes the formation of an opened P_4. This view is supported by the corresponding EH-calculations.

Scheme 2

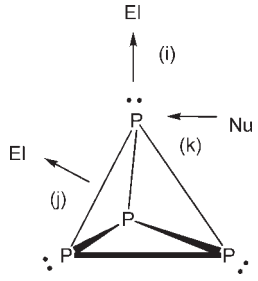

Scheme 3

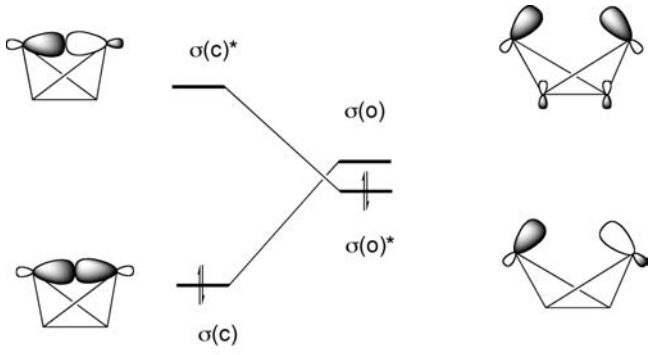

In the closed form, the tetrahedron **5c**, the PP-bonds form a bonding, σ(c) and an antibonding σ(c)* orbital, with a sizable energy splitting. In more detail the (T_d symmetrical) tetrahedron of white phosphorus possesses a more complicated orbital system, of which **5c** and **5o** are only a partial projection. In stretching one PP-bond the interaction with the central PP-π-bond comes to the fore. Such π-type interactions are already established for the perphospha-bicyclobutane.[14] For symmetry reasons, in **5o** the positive combination of orbitals, σ(o), is placed in energy *above* the antibonding combination, σ(o)*. It is the case of mingling of orbital interactions through space

(9) Kettle, S. F. A. *Theor. Chim. Acta* **1966**, *4*, 150–154.
(10) Jotham, R. W. *Chem. Soc. Rev.* **1973**, *2*, 457–474.
(11) Schmidtke, H. H. *Theor. Chim. Acta* **1968**, *9*, 199–209.
(12) Gimarc, B. M. *Molecular Structure and Bonding. The Qualitative Molecular Orbital Approach*; Wiley: New York, 1979.
(13) Schoeller, W. W. *Phys. Chem. Chem. Phys.* **2009**, *11*, 5273–5280.
(14) Schoeller, W. W.; Staemmler, V.; Rademacher, P.; Niecke, E. *Inorg. Chem.* **1986**, *25*, 4382–4385.

Table 1. Adiabatic S-T Energy Separations, $\Delta E_{S\text{-}T}$ ($E_S - E_T$), and Energy Differences (ΔE) between the Open and Closed Singlet States **5c** versus **5o**[a]

Level	$-\Delta E_{S\text{-}T}$ (**5o**)	$-\Delta E$ (**5c-5o**)
PBE-D/TZVP	−2.2	45.6
PBE-D/TZVPP	−2.0	46.9
RI-MP2/TZVP	2.7	50.9
RI-MP2/TZVPP	3.8	57.3
RI-CC2/TZVP	4.4	49.5
RI-CC2/TZVPP	4.8	55.2

[a] Values are in kcal/mol.

with orbital interactions through bond, well-known from the pioneering work of Hoffmann.[15] It must be noted here that phosphorus is valence isoelectronic to the CH fragment; thus, the same analysis can be applied to the ring-opening of tetrahedrane (C_4H_4) from T_d symmetry as well.[16]

The qualitative model was tested by quantum chemical calculations at various levels of sophistication. The results are summarized in Table 1.

At all levels of investigation (a) the adiabatic energy differences between both states (S and T) of **5o** result fairly small in energy, and (b) the closed form of P_4, **5c**, is essentially more stable than its open congener, **5o**. Some trends are apparent: the density functional calculations yield a preference for a triplet ground state, **5o**, while the MP2 and CC2 level calculations result in a singlet ground state. Moreover, MR-MCSCF calculation on **5o** with a 6-311++g(2d,p) bases (CAS(8,6) plus multireference correction at the MR-MP2 level) again facilitate a singlet ground state for **5o**, with a S-T energy difference of −1.8 kcal/mol. It ensures that the S-T energy separation is small, but a singlet is the ground state of the biradicaloid **5o**. At all levels of investigation the open form of P_4, **5o**, as well as the closed **5c**, are local energy minima; the latter is energetically favored over the former. The calculated energy difference results are larger with the (more flexible) TZVPP than the TZVP basis set; it agrees quite well with 51.3 kcal/mol for the splitting of one PP-bond as estimated from experiment.[17]

b. Frontier Orbitals of the Transition Metal Fragment and the 2:1 Approach. Within ligand field theory[18] the monocationic transition metal fragment **1** can be considered as a 16e-complex, with d^8 from the transition metal and further 8 electrons from the phosphorus lone pair ligands. Such species are quite stable entities, as it is well-known in the Wilkinson catalyst[19] or the Vaska and Di Luzio complex.[20] Typical for these species is the presence of a non-bonding d_{z^2}-orbital, shown for fragment **1** in Scheme 4.

Within the D_{2h} symmetry of the five d-orbitals at the transition metal center, the d_{xy} orbital can interact with the lone pair orbitals supplied by the phosphine ligands and form a strongly bonding and antibonding molecular orbital. The other sets of d-orbitals remain essentially

Scheme 4

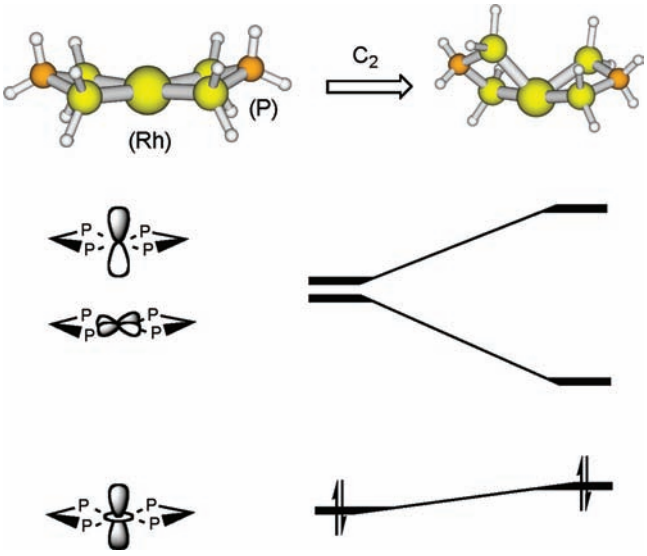

non-bonding; they do not match symmetry with the corresponding ligand orbitals. The highest occupied molecular orbital (HOMO) refers to the d_{z^2} orbital of the transition metal center. A full symmetry analysis of this aspect is summarized in the Supplement.

The lowest unoccupied molecular orbital (LUMO) is constituted (within D_{2h} symmetry) from the d_{xy} orbital, albeit antibonding with respect to the ligand orbitals. The LUMO+1 is close in energy and refers to a p-orbital at the transition metal center. Thus within this classification **1** is a nucleophilic *and* an electrophilic species. Noticeably, an easy conformational change in **1** from square planar to (pseudo) trigonal-bipyramidal coordination with an empty equatorial coordination site removes the planarity, by rotation around one P[M]P axis. While the dppm ligands can preserve their geometrical features (bond lengths, bond angles), this distortion dictates at the same time non-planarity on the structure. It changes the moiety according to C_2-symmetry; the resulting frontier orbitals possess like symmetry and can interact with each other. The LUMO orbitals split energetically into two orbitals, lower and higher in energy. The effect on the HOMO is much less pronounced. In other words, a simple C_2 distortion of the planar geometry increases the electrophilicity of this species. A conformational change, schematically indicated in Scheme 4, is in fact a low energy process. This gives rise to *conformational controlled philicity* in **1**, induced by easy structural changes. It is in contrast to the behavior of carbenes and silylenes, which have rigid structures, and an electrophilic and nucleophilic behavior in a reaction occurs in distinct different phases of the P_4 addition reaction.[13]

The density functional theory (DFT) calculations predict for the triad of transition metals, Rh, Ir, and to less extent for Co, sizable singlet−triplet (S-T) energy separations (Table 2).

The S-T energy separation value is smallest for **1-Co** but increases sizably for **1-Rh** and **1-Ir**. It is the consequence of the general increase of the ligand field splitting for the 4d/5d transition elements and reflects the well-known preference of these metals to form low spin rather

(15) Hoffmann, R. *J. Am. Chem. Soc.* **1968**, *90*, 1475–1485.
(16) Boehm, M. C.; Gleiter, R. *Tetrahedron Lett.* **1978**, *14*, 1179–1182.
(17) (a) Pauling, L.; Simonetta, M. *J. Chem. Phys.* **1952**, *20*, 29–34. (b) Moffitt, W. E. *Trans. Faraday Soc.* **1948**, *44*, 987–992.
(18) Cotton, F. A., *Chemical Applications of Group Theory*; John Wiley & Sons: New York, 1990.
(19) Osborn, J. A.; Jardine, F. H.; Young, J. F.; Wilkinson, G. *J. Chem. Soc. A* **1966**, 1711–1732.
(20) Vaska, L.; Di Luzio, J. W. *J. Am. Chem. Soc.* **1961**, *83*, 2784–2785.

Table 2. Adiabatic S-T Energy Separations at the PBE/TZVP Level for the Triad of Parent **1**, with M = Co, Rh, Ir

fragment	$-\Delta E_{S\text{-}T}$, in kcal/mol
1-Co	10.3
1-Rh	41.8
1-Ir	55.2

than high spin complexes. Interestingly, in experiments only reactions with the Rh- and Ir-derivatives have been reported; the Co-derivate has escaped so far from a clear characterization.[4] According to our calculations the fragment **1-Co** is less likely to be utilized as a stable fragment for studies of reactions with P_4.

The quantum chemical calculations indicate that a direct approach (**j**) (see Scheme 2) of the transition metal fragment to P_4 is energetically less favorable than an indirect approach via an (**i**) type intermediate. For the latter different possible approach paths were considered, as outlined in Scheme 5.

In **6** a monoadduct of [M] with P_4 is formed. Alternatively, it could add a second [M] into **7** or a second P_4 into **8**. If the electrophilic nature of **1** is prevailing, coordination takes place in the (i) approach, and the C_{3v} local symmetry of the P_4 unit is preserved. However, if the nucleophilic nature of the fragment **1** is dominant, in the approach to P_4 the (k) approach path is predicted. A third case may be considered here, **1** acts simultaneously as an electrophilic as well as a nucleophilic species by a superposition of both interactions. The bonding situation is sketched in Scheme 6.

In principle this analysis follows the Dewar−Chatt−Duncanson one on bonding of a transition metal fragment to a main-group fragment.[21] Since **1** as well as P_4 are closed shell species a possible mutual interaction between both fragment is expected to be weak.

All of the various possibilities were studied by the density functional calculations. In the investigations two different models were probed; (a) the phenyl groups in the dppm ligand were replaced by hydrogens, for the sake of clarity. This level is denoted here as parent; (b) alternatively, the full dppm substitution at the ligands was considered. Overall the highly flexible TZVP-basis of triple-ζ quality (triple-ζ) was used throughout. The PBE-density functional was at times supplemented by dispersion energy corrections. We restrict our considerations to a detailed analysis of the rhodium derivatives; it is the middle representative in the triad M = Co, Rh, Ir.

The relevant species on the electronic hypersurface are **6** and **7**. A pictorial representation of both is presented in Figure 1.

The most important structural parameters of both structures are collected in Table 3.

As revealed by the charges, Figure 1A, in **6** (parent compound) the transfer of electron density from the transition metal fragment to the P_4 unit is negligible. Thus **1-Rh** is bound to one corner of the tetrahedron by a balanced transfer of electron density toward P_4, accomplished by back-donation of almost the same amount. The M−P distance is 2.400 Å, and a corresponding Wiberg-bond index result is 0.2 (at times for the parent compound). The equilibrium distance for M−P in the parent compound and the dppm substituted molecule result are similar. As a further consequence of the forward plus back-donation of **1-Rh** to P_4 the resulting equilibrium geometry is given by a superposition of the (i) approach (El) and (k) approach (Nu), and the valence angles $\angle MP_\alpha P_\beta$ are different, rather than equal in magnitude (see Table 1).

The effect on the $P_\alpha P_\beta$ bond length is negligible, but the bonding situation is somewhat different for the equilibrium geometry of **7**. The Wiberg bond index (for the parent compound) is again fairly small (0.2), which precludes a transition metal−phosphorus single bond. Since the extent of charge-transfer to the P_4 unit in **7** is larger than in **6**, a stronger emphasis is given on approach path (k) (Scheme 3), with the consequence of stretching of one P−P bond in the tetrahedron.

Because **7** possesses a stretched PP-bond one expects a biradicaloid character, as anticipated from the discussion in section a. Quantum chemical investigations confirm this assertion; for **7** (parent) the energy lowest triplet state result is 21.4 kcal/mol above the singlet ground state. Monocoordination into (parent) **6** is exothermic; most noticeable it can further coordinate a second P_4, with formation of (parent) **7**. The alternative path leads from **6** to (parent) **8**. It results in a species which is not stable upon dissociation, and formation of **6** plus P_4 is obtained. Further studies reveal that the dppm substituted **6-Rh** adds a second **1-Rh** without energy barrier; however, the resulting electronic hypersurface is very flat.

Some words on the steric crowding in the equilibrium structures are appropriate. Steric demand is not of importance in the monocoordinated species **6**. The phenyl groups of the ligand can easily wrap the P_4. It is, however, a problem in **7**. As the plots indicate (Figure 1, C) the structure has to encounter steric congestion to form dicoordination at P_4.

A further understanding of this aspect in the compounds **6** and **7** is provided by the reaction energies, given in the eqs 1 to 3.

$$\mathbf{1} + P_4 \Rightarrow \mathbf{6} + \Delta E \quad (1)$$

$$\mathbf{6} + \mathbf{1} \Rightarrow \mathbf{7} + \Delta E \quad (2)$$

$$2\times(\mathbf{1}) + P_4 \Rightarrow \mathbf{7} + \Delta E \quad (3)$$

Reaction 1 refers to addition of cationic transition metal fragment to one P_4, while in reaction 3 two **1**'s are added. Reaction 2 yields the energy balance for addition of one further P_4 to the already formed monoadduct **6**. The energy balances were computed at the PBE-D level, which include dispersion corrections for the bulky substituents attached at **1**. The results are summarized in Table 4.

The results obtained for the hydrogen substituted cationic fragment **1** differ considerably from those for the dppm-substituted **1-Rh**. The former can be considered as the model system while the latter is the real substituted molecule, probed in the experimental investigations. A hint for the understanding of the essential different energy balances for the reactions 1 to 3 is provided by the dispersion energies, ΔE_{disp}. Their contributions on the reactions are sizable for the dppm substituted derivatives.

(21) (a) Dewar, M. *Bull. Soc. Chim. Fr.* **1951**, *18*, C79. (b) Chatt, J.; Duncanson, L. A. *J. Chem. Soc.* **1953**, 2939. (c) Chatt, J.; Duncanson, L. A.; Venanzi, L. M. *J. Chem. Soc.* **1955**, 4456–4460.

Scheme 5

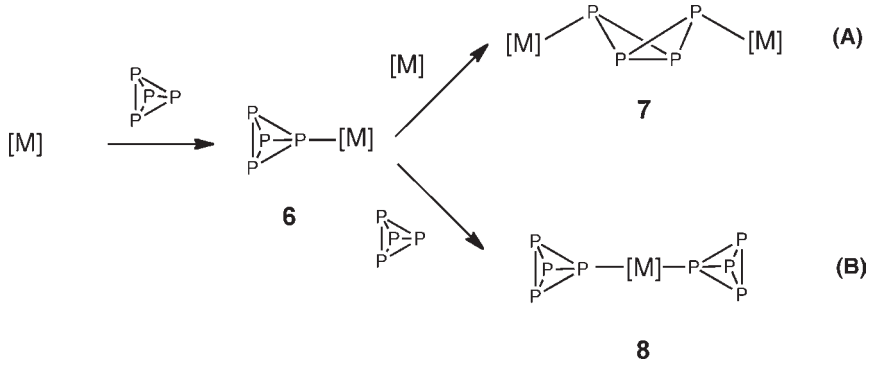

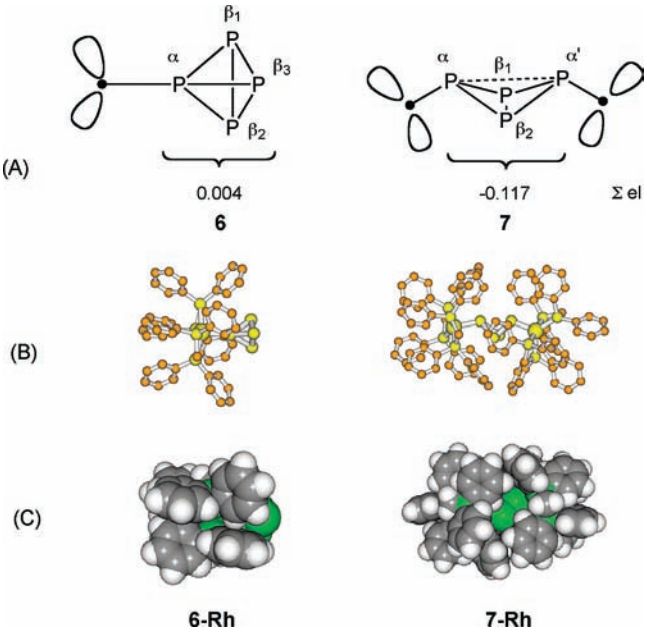

Figure 1. (A) NBO charges of parent monocationic **6** (left) and dicationic **7** (right), summarized over the P_4 unit of the parent structures. (B) Ball and stick models of the equilibrium geometries of dppm-substituted structures (hydrogen atoms are omitted, and (C) space-filling models.

Scheme 6

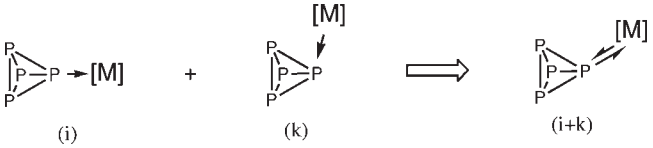

In the DFT approach with inclusions of van der Waals interactions[22] the energy is given by eq 4, the sum of the energy of the density functional, E_{mean}, plus the energy, E_{disp}, for the dispersion energy corrections.

$$E = E_{mean} + E_{disp} \quad (4)$$

As has been shown in the early days of quantum mechanics by London et al.[23] that van der Waals forces are long-range in character, hence they contribute for the mutual interactions in bulky systems.[24] The ligand **1-Rh** is substituted with 4 phenyl groups, and one expects mutual interactions. The π-stacking of benzene has been studied in the experiment, and the benzene dimer energy result is 2.4 kcal/mol.[25] A variety of quantum chemical investigations are in support of these experimental findings.[26]

In more detail, reaction 1, which refers to monoaddition of the cationic fragment to P_4, is exothermic for the parent as well as for dppm-substituted **1-Rh**. According to the calculations **6** is formed from its constituents without an energy barrier. Its stability is larger for the dppm substituted **1** than for the parent compound. In forming **6-Rh**, the dispersion energy corrections ΔE_{disp} are sizable, which indicates van der Waals interaction of the phenyl groups at **1-Rh** with the phosphorus atoms of the P_4 unit. The effect is even more pronounced for the reaction 3

Table 3. Most Important Structural Parameters of **6** and **7**[a]

parameter **6**	parent **6**	dppm **7**	parent **7**	dppm
M−P	2.400	2.332	2.438, 2.438[b]	2.364, 2.404[b]
∠MP(α)P(β_1)	150.1	151.2	121.6	133.7
∠MP(α)P(β_2)	148.6	147.3	116.0	127.7
∠MP(α)P(β_3)	123.4	131.6	173.6	166.7
P(α)P(β)	2.230−2.240	2.232−2.236	2.236, 2.252, [2.348][c]	2.234, 2.253, [2.330][c]

[a] Bond lengths are in Å, bond angles in degrees. [b] The first value is for M−P(α), second value for M−P(α′). [c] In brackets values, for axial bond P(α)P(α′).

Table 4. Energy Balances for Reactions 1 to 3 for the Parent and dppm Substituted Structures[a]

reaction	substituent	$-\Delta E$ (kcal/mol)	$-\Delta E_{disp}$ (kcal/mol)
1	parent	18.2	5.7
	dppm	27.1	17.0
2	parent	−15.1	7.2
	dppm	1.0	35.1
3	parent	3.1	12.9
	dppm	28.1	52.1

[a] Relative energies ΔE are in kcal/mol; ΔE_{disp} values refer to the corrections for dispersion energies.

(22) (a) Antony, J.; Grimme, S. *Phys. Chem. Chem. Phys.* **2006**, *8*, 5287–5293. (b) Grimme, S. *J. Comput. Chem.* **2006**, *27*, 1787–1799.

(23) (a) Eisenschitz, R.; London, F. *Z. Physik* **1930**, *60*, 491. (b) London, F. *Z. Physik* **1930**, *63*, 245.

(24) (a) Schoeller, W. W. *Theor. Chem. Acc.* **2010**, *127*, 223–229. (b) Schoeller, W. W. *J. Mol. Struct. THEOCHEM* **2010**, *957*, 66. (c) Jutzi, P.; Mix, A.; Neumann, B.; Rummel, B.; Schoeller, W. W.; Stammler, H.-G.; Rozhenko, A. B. *J. Am. Chem. Soc.* **2009**, *131*, 12137–12143.

(25) Grover, J. R.; Walters, E. A.; Hui, E. T. *J. Phys. Chem.* **1987**, *91*, 3233–3237.

(26) Waller, M. P.; Robertazzi, A.; Platts, J. A.; Hibbs, D. E.; Williams, P. A. *J. Comput. Chem.* **2006**, *27*, 491–504 and references herein.

Scheme 7

Scheme 8

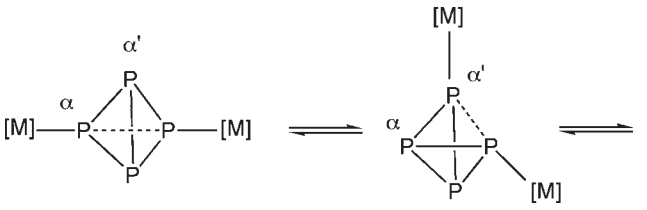

when two fragments are now attached to the central P_4 tetrahedron. The calculations indicate that the stability of **7-Rh** may be attributed to the gain in π-stacking energy among the phenyl rings, plus additional van der Waals energy with the central P_4-unit. A similar situation is also pronounced for the reaction 2. For the parent compound the dissociation of **7** into **6** plus **1** is exothermic, and the second transition metal fragment is only weakly bound to **6**. Further calculations reveal that the parent **7** has only a marginal energy barrier ($\approx$ 2 kcal/mol) for dissociation of one fragment **1**. The situation is somewhat different for the dppm substituted **7-Rh**. Because of the large van der Waals forces in **7-Rh**, dissociation into **6-Rh** plus **1-Rh** is slightly endothermic, albeit to a negligible extent.

On this basis one can describe **7-Rh** in equilibrium with **6-Rh** plus **1-Rh**, schematically sketched in Scheme 7. The fact that the transition metal complex **7** is held together by only weak binding forces of **1** to the P_4 tetrahedron has further consequences (Scheme 8). The transition metal fragments can easily change its coordination site at the P_4. The quantum chemical calculations, based on a detailed surface scan, predict for this process an upper energy barrier of $\approx$3 kcal/mol.

c. Formation of 3-Rh. Formally compound **3** can be derived from **6** and/or **7**. The quantum chemical calculations indicate that such a process occurs from the mono-adduct **6**. There are two reasons for this assertion: (a) the steric demand of the bulky dppm ligands is larger in **7** than in **6**. Thus steric congestions in the rearrangement reactions, induced by conformational changes, are more accounted for in the former than in the latter structure. (b) The P_4 moiety has gathered more electron density in **7** than in **6**, a disadvantage for transition state formation (see vide infra). Species **6** is easily accessible since **6** and **7** can be considered in equilibrium (Scheme 6). We have calculated the reaction path for the parent compound of **6**. The structures of the stationary points as well as the equilibrium geometry of the product **3-Rh** are summarized in Figure 2.

The transition state **TS** of the reaction refers to a flattened transition metal fragment weakly interacting with the P_4-moiety, and the P_α-$P_{\alpha'}$ bond is only slightly lengthened. Thus according to the qualitative rules depicted in Scheme 1, the transition state structure refers to a loose complex of a predominantly nucleophilic **1** with P_4. Upon a conformational change of the ligand (see Scheme 1) the electrophilicity of the transition metal fragment **1** is considerably enhanced, and a low-energy insertion process takes place. Overall the energy barrier for the

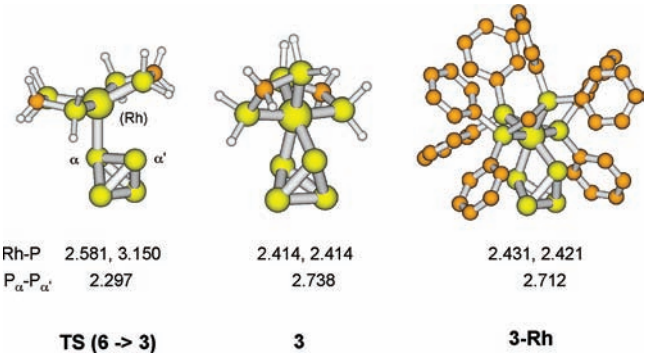

Figure 2. Ball and stick plots of the stationary points for the reaction of **6** to **3**. For the dppm substituted product the hydrogen atoms are omitted for clarity. Bond lengths are in Å units.

Scheme 9

insertion process result in 4.3 kcal/mol, and the reaction from **6** to **3** is exothermic by −9.9 kcal/mol. Energy optimization at the same computational level (PBE-D/TZVP) reveals for **3-Rh** a structure well in agreement with the experimentally determined X-ray investigations.[4] As known from silylene chemistry[24a] electrophilic addition (approach (j), see Scheme 2) forms by a direct path to the insertion product **3**. For the case studied at hand such an approach path could not be detected by the quantum chemical calculation and is obviously essentially higher in energy than the formation of an equilibrium of **6** with **7**, which crops up without energy barrier from 1 P_4 and 2 TM-fragments **1**.

d. Formation of 4 and the j-Step Formalism. The experimentally observed species **4** differs from the other species discussed so far in that a ring expansion in the ligand species **1** takes place. We have also investigated this reaction by means of DFT calculations. In fact a two-step mechanism is responsible for this reaction: first, a ligand from the transition metal fragment dissociates; second, a subsequent isomerization reaction of the P_4-moiety; and third, an association of the ligand to the rearranged P_4-moiety takes place. We may call this a j-step mechanism, in contrast to the approach path (j) for the transition metal fragment to P_4. Formally, ligand dissociation leads to a 14e-species, which are considered as highly reactive species.[27]

For the isolated cationic **1**, ligand dissociation is a high energy process. This is revealed by a comparison of the following two structures (Scheme 9). In **1a** and in **1b** one and/or two ligands are dissociated from the coordination site. The former structure is higher in energy by 25.6 kcal/mol than **1** and the latter even by 50.0 kcal/mol. This precludes ligand dissociation as a low-energy process in the free transition metal fragment **1**. The situation is,

(27) Romero, P. E.; Piers, W. E. *J. Am. Chem. Soc.* **2007**, *129*, 1698–1704.

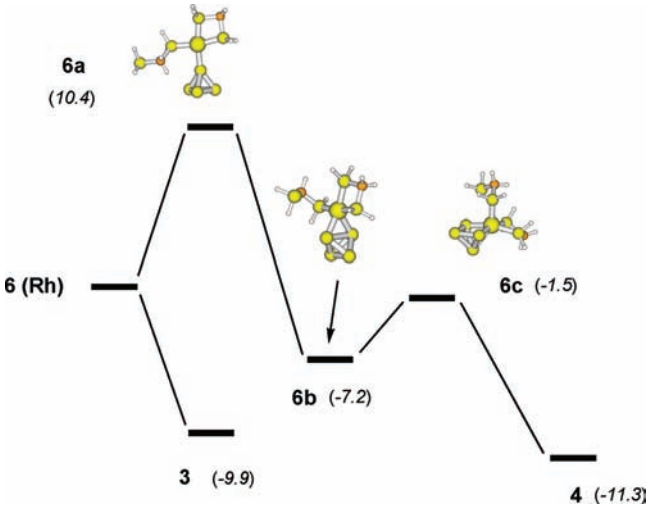

Figure 3. Cascade of isomerization reactions after the j-step reaction of monocationic **6**; the graphical plots refer to the equilibrium geometries of the investigated species during the isomerization reaction. Values in parentheses (italics) refer to relative energies in kcal per mole, with respect to **6** (Rh).

however, different if **1** is already coordinated at one corner of the P_4 tetrahedron, as it is the case in **6**. A cascade of reactions is now induced, as summarized in Figure 3.

All of these species are distinct energy minima on the hypersurface, but are separated from each other by only small energy barriers. They are in the range of 1−2 kcal/mol, thus negligible quantities even at low temperature. Hence these will not be listed here in detail. The loss of one ligand, as in **6a**, is the rate-determining step in the overall process. It requires simple bond stretching of one Rh−P bond and in concert the Rh−P bond to the P_4 moiety is shrunk to 2.301 Å. A 1,2-reaction of the metal-fragment leads easily to **6b**. This species is fairly stable (−7.2 kcal/mol with respect to **6**) by forming a three-center bond with P_4. The bridged PP-bond is elongated to 2.499 Å while the Rh−P bonds become elongated (2.375 and 2.384 Å). Although **6b** is in a sink, it again is unstable. The metallacycle **6c** is the next intermediate in this cascade mechanism. It is obtained by bending the bridging transition metal fragment over to one of the distal phosphorus atoms. Finally, the free ligand adds at one phosphorus center of the four-membered ring, over facile bipyramid formation the product **4** is formed. Interestingly, a direct route from **6b** to **3** could not be found. It would require that the free donor ligand attacks the bridged P−P bond. Such an approach is overall too energy costly.

The proposed cascade mechanism seems independent of the substituents. For their evaluation the hydrogens (at all positions) were replaced by methyl groups. The j-step from **6** to **6a** appears larger (19.6 kcal/mol); it indicates that a dimethylamino substituent is more strongly bound to the transition metal than the amino group. Again the overall reaction to **4** results in an energetic sink and is −12.6 kcal/mol more stable than **6**.

In essence the cascade mechanism is induced by the initial j-step reaction of one ligand in the monoadduct. It is the process with the highest energy demand. The relative energies for the various stationary points on the electronic hypersurface may be mediated by the phenyl-substituents at the phosphorus atom (in the ligands), but it is to be expected that the overall mechanism proposed by these model calculations will not essentially change. In general the reactions should proceed with small energy barriers, which can be easily mastered at low temperature. The considerations imply that further reactions occur from the monoadduct **6**. This seems plausible; it is the steric congestion in **7-Rh** that inhibits further distortion of one ligand required to initiate a reaction. The equilibrium between both species (Scheme 7) allows easy dissociation of the dimeric adduct **7** into the monoadduct **6**.

One further structural alternative to **7** is **9**; it refers to the dicationic insertion of a second transition metal fragment in **3** into the PP-bond, distal to the first transition metal center. Its equilibrium structure is schematically shown in Scheme 10.

Such a dicationic species has been predicted as transient in the report of Yakhvarov and Peruzzini et al.[28] However stable dications in phosphorus chemistry are well-known,[29] and structure **9** results −18.2 kcal/mol more stable than **7** on the hypersurface. Since **7** (R = H) is unstable with respect dissociation into **6** plus **1** by −15.1 kcal/mol (see Table 4) it is only −3.0 kcal/mol more stable than the reference compound **6** plus separated **1** (Figure 3). Thus our considerations make **9** unlikely to appear as a stable intermediate on the electronic hypersurface. In accordance with the experimental investigations, **3** and **4** are overall the most stable species for the reaction.

Theoretical Section

Calculations were performed with the GAUSSIAN suite of programs (G03)[30] and the TURBOMOLE 6.0 set of program system.[31] Stationary points were determined by energy minimization without symmetry constraints. Since the electronic hypersurfaces at the transition state regions are very flat, corresponding energy maxima were obtained by detailed surface scans. These also confirm the proper connection between educts and products. The TZVP-basis set[32] is of triple-ζ quality and was utilized for all investigated structures. In some cases, for the evaluation of the opened versus closed P_4,

(28) Suggested structure **2** in ref 4.

(29) (a) Weigand, J. J.; Holthausen, M.; Fröhlich, R. *Angew. Chem., Int. Ed.* **2009**, *48*, 295–298. (b) Weigand, J. J.; Burford, N.; Lumsden, M. D.; Decken, A. *Angew. Chem., Int. Ed.* **2006**, *45*, 6733–6737.

(30) Frisch, M. J.; Trucks, G. W.; Schlegel, H. B.; Scuseria, G. E.; Robb, M. A.; Cheeseman, J. R.; Montgomery, Jr., J. A.; Vreven, T.; Kudin, K. N.; Burant, J. C.; Millam, J. M.; Iyengar, S. S.; Tomasi, J.; Barone, V.; Mennucci, B.; Cossi, M.; Scalmani, G.; Rega, N.; Petersson, G. A.; Nakatsuji, H.; Hada, M.; Ehara, M.; Toyota, K.; Fukuda, R.; Hasegawa, J.; Ishida, M.; Nakajima, T.; Honda, Y.; Kitao, O.; Nakai, H.; Klene, M.; Li, X.; Knox, J. E.; Hratchian, H. P.; Cross, J. B.; Bakken, V.; Adamo, C.; Jaramillo, J.; Gomperts, R.; Stratmann, R. E.; Yazyev, O.; Austin, A. J.; Cammi, R.; Pomelli, C.; Ochterski, J. W.; Ayala, P. Y.; Morokuma, K.; Voth, G. A.; Salvador, P.; Dannenberg, J. J.; Zakrzewski, V. G.; Dapprich, S.; Daniels, A. D.; Strain, M. C.; Farkas, O.; Malick, D. K.; Rabuck, A. D.; Raghavachari, K.; Foresman, J. B.; Ortiz, J. V.; Cui, Q.; Baboul, A. G.; Clifford, S.; Cioslowski, J.; Stefanov, B. B.; Liu, G.; Liashenko, A.; Piskorz, P.; Komaromi, I.; Martin, R. L.; Fox, D. J.; Keith, T.; Al-Laham, M. A.; Peng, C. Y.; Nanayakkara, A.; Challacombe, M.; Gill, P. M. W.; Johnson, B.; Chen, W.; Wong, M. W.; Gonzalez, C.; and Pople, J. A. *Gaussian 03*, Revision C.02; Gaussian, Inc.: Wallingford, CT, 2004.

(31) (a) Ahlrichs, R.; Bär, M.; Häser, M.; Horn, H.; Kölmel, C. *Chem. Phys. Lett.* **1989**, *162*, 165–169. (b) Ahlrichs, R.; Arnim, M. In *Methods and Techniques in Computational Chemistry: MET ECC-95*; Clementi, E., Corongiu, G., Eds.; STEF: Cagliari, 1995; p 509 ff; http://www.cosmologic.de/QuantumChemistry/main_turbomole.html.

(32) Schäfer, A.; Huber, C.; Ahlrichs, R. *J. Chem. Phys.* **1994**, *100*, 5829–5835.

Scheme 10

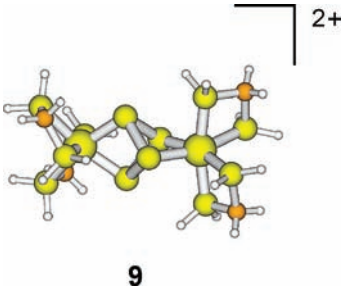

9

the more elaborate TZVPP-basis set[31] was added. As density functional the PBE (Perdew, Burke, Ernzerhof) functional[33] was employed. For the calculation of the bulky structures the account for dispersion energies (van der Waals interaction) is mandatory. We have used here the Grimme approach,[22] as implemented in the TURBOMOLE program system. Since the dispersion corrections are not assigned for Ir, the quantum chemical studies were restricted to the Rh-derivatives, hydrogen and phenyl substituted structures as well. The resolution of the identity (RI)[34] was used within the TURBOMOLE program. The MP2 as well as the CC2[35] calculations were performed without further calibration. The population analysis followed the natural orbital scheme.[36] The MOLDEN program packet was utilized for drawing the various stationary points determined from the computations.[37] The MCSCF calculations were performed with the GAMESS program system,[38] and the subsequent MR-MP2 calculations according to the method described by Hirao.[39] The equilibrium coordinates of the relevant phenyl-substituted species are collected in the Supporting Information.

Conclusions

The results of these investigations can be summarized as follows:

(1) The triad of the transition metals M = Co, Rh, Ir forms cationic stable species with the dppm ligands. The adiabatic S-T energy separations are sizable for **1-Rh** and **1-Ir**, but less for **1-Co**. The latter can be considered as a biradicaloid species. The Cobalt(I) species, that is, $[Co(dppm)_2]^+$ does not exist while the Rh- and Ir-representatives of **1** are useful targets for reaction with white phosphorus.

(2) In the further investigations only the Rh-derivative was studied in detail. In the planar confirmation the HOMO is the d_{z^2} orbital, as is known from classical 16e species, for example, the Wilkinson catalyst. The LUMO consists of an almost degenerate pair of orbitals. Upon conformational change the LUMO orbitals will strongly mingle with each other, and the fragment enhances its electrophilicity. We may coin this as conformational philicity control in the transition metal fragment.

(3) Consequently, the insertion process of **1** leading to **3**, which has been characterized experimentally for **3-Ir**, is a low energy process. The fragment increases its electrophilicity in the transition state region by a conformational change.

(4) The species **4** is achieved by a j-step mechanism; **1** coordinates first into a σ-complex to **6**, followed by ligand dissociation (j-step) and subsequent reaction over a cascade of intermediates to the final product **4**. The various intermediates rearrange to each other over negligible energy barriers. The rate determining step is the ligand dissociation in the intermediary formed monoadduct with P_4.

(5) The precursor for the reaction to **4** is **6**, which is in equilibrium with its 2:1 dimer, **7**. It is formed by reaction of 2 fragments **1** with one molecule P_4. The quantum chemical calculations indicate that this species is considerably stabilized by the π-stacking interaction of the benzene rings at the phosphorus atoms.

Overall, the investigations reveal very flat potential energy surfaces, which are mediated by the substituents attached at the ligands. The present quantum chemical treatment refers to calculations for the gas phase. Inclusion of solvent effects can be expected to induce changes in the relative energies of some of the reaction or species involved, in particular where changes in the relative energies of some of reactions or species are concerned, like those described in eqs 1−3. However, the investigations may serve as a first understanding to the reactivity of transition metal fragments with white phosphorus, as it is documented in the vast experimental reports in this scientific area.

Acknowledgment. The author thanks the University of Riverside for support, Dr. Toensing for computational help, Dr. G. D. Frey and Prof. T. Morton for fruitful discussions, and the Theoretical Chemistry group at the University of Bielefeld for generous allocation of computer time.

Supporting Information Available: Further details about the parent compound **1**, and the equilibrium structures of **1-Rh** and **6-Rh**. This material is available free of charge via the Internet at http://pubs.acs.org.

(33) Perdew, J. P.; Burke, K.; Ernzerhof, M. *Phys. Rev. Lett.* **1996**, *77*, 3865–3868.
(34) Weigend, F.; Häser, M. *Theor. Chim. Acc.* **1997**, *97*, 331–340.
(35) Christiansen, O.; Koch, H.; Jørgensen, P. *Chem. Phys. Lett.* **1995**, *243*, 409–418.
(36) (a) Foster, J. P.; Weinhold, F. *J. Am. Chem. Soc.* **1980**, *102*, 7211–7218. (b) Reed, A. E.; Weinhold, F. *J. Chem. Phys.* **1983**, *78*, 4066–4073.
(37) Schaftenaar, G.; Noordik, J. H. *J. Comput. Aided Mol. Des.* **2000**, *14*, 123–134.
(38) Schmidt, M. W.; Baldridge, K. K.; Boatz, J. A.; Elbert, S. T.; Gordon, M. S.; Jensen, J. H.; Koseki, S.; Matsunaga, N.; Nguyen, K. A.; Su, S. J.; Windus, T. L.; Dupuis, M.; Montgomery, J. A. *J. Comput. Chem.* **1993**, *14*, 1347–1363.
(39) Hirao, K. *Chem. Phys. Lett.* **1992**, *190*, 374–380.